

Naphthyl-fused phosphepines: Luminescent contorted polycyclic P-heterocycles

Thomas Delouche, Réka Mokrai, Thierry Roisnel, Denis Tondelier, Bernard Geffroy, László Nyulászi, Zoltán Benkő, Muriel Hissler, Pierre-Antoine Bouit

▶ **To cite this version:**

Thomas Delouche, Réka Mokrai, Thierry Roisnel, Denis Tondelier, Bernard Geffroy, et al.. Naphthyl-fused phosphepines: Luminescent contorted polycyclic P-heterocycles. 2019. cea-02318890

HAL Id: cea-02318890
https://cea.hal.science/cea-02318890

Preprint submitted on 17 Oct 2019

HAL is a multi-disciplinary open access archive for the deposit and dissemination of scientific research documents, whether they are published or not. The documents may come from teaching and research institutions in France or abroad, or from public or private research centers.

L'archive ouverte pluridisciplinaire **HAL**, est destinée au dépôt et à la diffusion de documents scientifiques de niveau recherche, publiés ou non, émanant des établissements d'enseignement et de recherche français ou étrangers, des laboratoires publics ou privés.

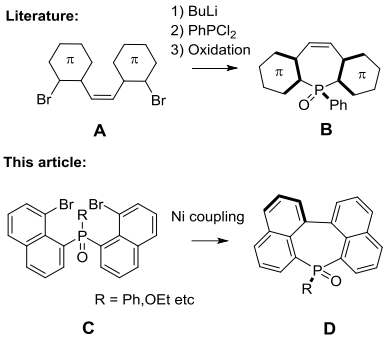
Naphthyl-fused phosphepines: Luminescent contorted polycyclic P-heterocycles

Thomas Delouche,[a] Réka Mokrai,[a,b] Thierry Roisnel,[a] Denis Tondelier,[c] Bernard Geffroy,[d] László Nyulászi,[b,e] Zoltán Benkő,*[b] Muriel Hissler*[a] and Pierre-Antoine Bouit*[a]

Abstract: the article presents the synthesis of a new family of naphthyl-fused phosphepines through Ni-mediated C-C coupling. Interestingly, the chloro-phosphine-oxide intermediate shows strong resistance toward oxidation/hydrolysis due to a combination of steric hindrance and pnictogen interactions. However it can undergo substitution reactions under specific conditions. The optical / redox properties and the electronic structure of these new π-systems were studied experimentally (UV-vis absorption, emission, cyclic voltammetry) and computationally (TD-DFT calculations, NICS investigation). Taking advantage of the luminescence of these derivatives, a blue emitting OLED has been prepared highlighting that these novel π-conjugated P-heterocycles appear as promising building blocks for solid-state lightning applications.

Introduction

During the last two decades, the research on phosphorus-containing π-conjugated systems based on small molecules, oligomers and polymers has increased substantially thanks to the development of "plastic electronic" devices.[1] Compared to purely organic π-systems, the presence of a heteroatom such as phosphorus affords multiple molecular engineering strategies in order to tune the chemical structure and the physico-chemical properties. Indeed, the P-atom can be involved in various bonding situations (σ^3,λ^3-phosphane, σ^2,λ^3-phosphaalkene, σ^1,λ^3-phosphaalkyne etc), which strongly impacts the nature of the delocalization in the corresponding π-system.[2] Furthermore, the specific reactivity of the σ^3,λ^3-P-atom affords an almost unlimited way of tuning its properties. [3] Among these strategies, introducing the P-center into an unsaturated ring is also an excellent way to modify the properties of the corresponding π-system. Phosphole, the P-analogue of thiophene, is by far the most studied P-heterocycle based π-system from the point of view of its reactivity as well as for its introduction into devices (light-emitting diodes, solar cells, batteries…).[4] However, P-heterocycles are not limited to the phosphole family and during the last few years, other π-systems based on phosphetenes (4-membered unsaturated P-ring),[5] phosphaphenalenes / phosphinines (6-membered P-ring)[6] or phosphepines (7 membered P-rings)[7] have started to be studied in the context of molecular materials. The phosphepine ring caught our attention as it displays the most distorted framework among these conjugated heterocycles, which may strongly impact the physico-chemical properties. In particular, we and others studied non-planar diarylophosphepines (**B**, Scheme 1) showing tunable optical/redox properties and promising activity in field-effect transistors.[8] Those diarylophosphepines are usually synthesized according to a classical sequence of dilithiation of a dibromoaryl then reaction with a dichlorophosphine (Scheme 1). In order to develop a new family of π-extended-phosphepine, we decided to adapt the Ni-mediated coupling strategy that allowed M. Wagner *et al* to prepare distorted borepins and thus investigate the effect of the insertion of a P-atom into such quadruply-fused phosphepine **D** (Scheme 1).[9] In this article, we present the synthesis of a new family of naphthyl-fused phosphepines. The optical and redox properties and the electronic structure of these new π-systems have been studied experimentally and computationally. Incorporation of one of these molecules into an OLED device has also been performed.



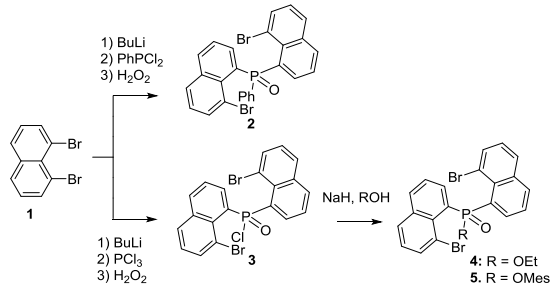
Scheme 1. Reported access to π-extended phosphepine (**B**) and synthetic strategy employed in this article.

[a] T. Delouche, R. Mokrai, T. Roisnel, Prof. M. Hissler, Dr P.-A. Bouit
Univ Rennes, CNRS, ISCR - UMR 6226, F-35000 Rennes.
E-mail: muriel.hissler@univ-rennes1.fr, pierre-antoine.bouit@univ-rennes1.fr
[b] Department of Inorganic and Analytical Chemistry, Budapest University of Technology and Economics Szt. Gellert ter 4 H-1111 Budapest, Hungary
E-mail: zbenko@mail.bme.hu
[c] LPICM, CNRS, Ecole Polytechnique, IPParis, 91128 Palaiseau, France
[d] *LICSEN, NIMBE, CEA, CNRS, Université Paris-Saclay, CEA Saclay, 91191 Gif-sur- Yvette Cedex, France*
[e] MTA-BME Computation Driven Chemistry Research Group. Szt. Gellert ter 4 H-1111 Budapest, Hungary
E-mail: nyulaszi@mail.bme.hu

Results and Discussion

Synthesis and structural study of precursors

Based on our synthetic strategy toward **D** (Scheme 1), the first step of our approach was the preparation of the bromonaphthyl-phosphines **C**. The reaction between 1,8-dibromonaphthalene **1** and BuLi followed by *in situ* addition of dichlorophenylphosphine and subsequent oxidation afforded quantitatively a product characterized by a single peak in the ^{31}P NMR spectrum (δ = +42.9 ppm) and broad multiplets in the ^{1}H NMR (Fig. S8). This phenomenon is due to the presence of interconverting rotamers at room temperature (rt). Indeed, the signals in the ^{1}H NMR sharpened upon cooling the temperature to 243K (Fig. S8).[9] The product was unambiguously characterized as **2** by its crystallographic structure (Scheme 2 and Fig. 1). The molecular structure of **2** displays high steric hindrance with torsion of the naphthyl ring as well as presence of intramolecular contacts shorter than the sum of van der Waals radii (d_{vdW}) between O and Br (3.122 Å <d_{OBr}<3.144 Å, see Fig 1, d_{vdW}(O-Br)=3.37 Å) and especially between P and Br centers Br (3.246 Å <d_{PBr}<3.399 Å, see Fig 1, d_{vdW}(P-Br)=3.65 Å). This sterically crowded structure with intramolecular interactions can explain the presence of interconverting rotamers at rt.



Scheme 2. Syntesis of bromonaphthyl substituted phosphine oxide **2**-**4**.

The same sequence was then performed using PCl_3 as starting phosphine and the product identified after oxidation was the chlorophosphine oxide **3** (Scheme 2). This compound displays similar NMR behaviour as **2** with broad ^{1}H signals that resolved upon cooling to temperature (Fig. S9). Furthermore, X-ray diffraction allowed the unambiguous characterization of **3** (Fig. 1). The high steric hindrance around the P-atom combined with the presence of intramolecular short contacts (3.204 Å <d_{OBr}<3.300 Å, 3.246 Å <d_{PBr}<3.399 Å, Fig 1) probably allows sterically protecting the P-Cl bond making **3** fully air and moisture stable. This is surprising because chlorophosphine-oxides are usually sensitive to hydrolysis. Nevertheless, the Cl atom of **3** could be substituted by alkoxides/aryloxides to afford **4** and **5** (Scheme 2). Their structures could be confirmed by X-ray diffraction (Fig S13-14).

In order to gain more insight into the nature of the weak interactions we have performed DFT calculations at different levels, here only the results obtained at the B3LYPD3/6-31+G* level are discussed. To estimate the energetic stabilization caused by these interactions, the corresponding isodesmic reaction depicted in Scheme S1 has been calculated for compounds **2** and **3**. Remarkable stabilization reaching 18.5 kcal/mol is found in **3**, while somewhat smaller but still significant value of 14.8 kcal/mol is obtained for **2**. The covalent character of possible P···Br and O···Br interactions has been assessed employing Wiberg Bond Indices (WBI). This shows practically no interaction between the O and Br centers (WBI:~0.007), whereas the WBI value for both P-Br pairs in the range of ~0.02 may indicate pnictogen interaction between P and Br.[10 - 11] The presence of weak interactions between the P and Br atoms is further corroborated by an atoms in molecules (AIM) analysis of the electron density (see ESI, Fig S25). In conclusion, a weak pnictogen interaction between P and Br may contribute to the particular stability of **3**, that can be easily handled in air and purify with classical chromatography techniques.

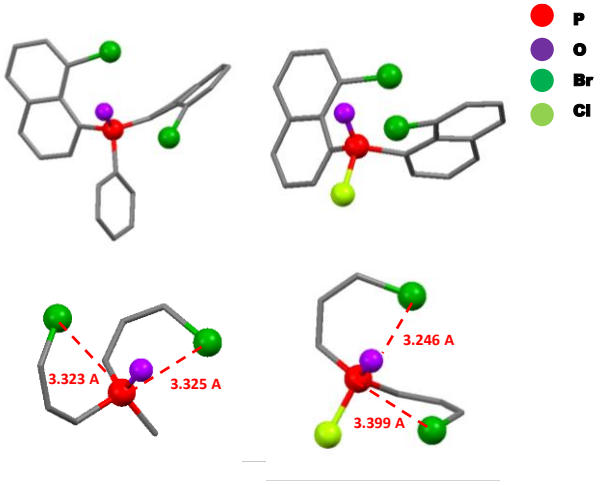
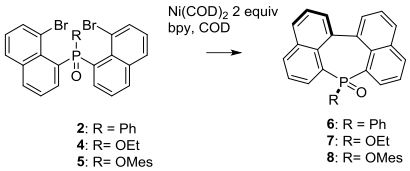


Figure 1: Crystallographic structures of **2** (left) and **3** (right) (top) with zooms on the P environment with measured P-Br distances (red dotted line) (down). Hydrogen atoms were omitted for clarity.

Synthesis and structural study of naphthyl-fused phosphepines

The fusing step toward **D** (Scheme 1) was then tested employing the Yamamoto-type conditions optimized by Wagner *et al.* [9] using 2 equiv. of $Ni(COD)_2$, COD (2 equiv.) and bpy in THF allowed us to convert **2** into **6** (^{31}P NMR: δ = +22.7 ppm) in good yields (75%) (Scheme 4). **5** was characterized by multinuclear NMR, HRMS and X-ray diffraction (Fig. 2). Based on these results, the Ni-mediated coupling was used to prepare **7**-**8** in good yields (75% and 47%, respectively). These examples show that the Yamamoto-type reaction is an efficient way to prepare unprecedented naphtyl-fused phosphepines from the corresponding bromo-naphthylphosphines. As expected for contorted polycyclic aromatic systems, the solubility of these

compounds in most organic solvents (DCM, AcOEt, THF…) is rather good.



Scheme 4. Synthesis of naphthyl-fused phosphepines **6-8**

Additionally, **6** and **8** were also characterized by X-ray diffraction. They both show similar structural features (Table 1) so the following paragraph will only detail **6**. The P-C bonds lengths are classical for phosphine-like structures ($d_{P\text{-}C}$ = 1.79-1.81 Å). In the 7-membered P-ring, all C-C bonds belonging to the naphthalene moiety are within the aromatic C-C distances (1.42 Å< d< 1.44 Å) while C3-C4 has clearly a single bond character (d = 1.513 Å). **6** displays a highly distorted C-backbone as illustrated by the $C_{13}C_3C_4C_{20}$ torsion angle of 38.9°. The distorted nature of the polycyclic framework in **6**-**8** is also verified by DFT calculations in the gas phase and the calculated characteristic distances and angles clearly match the experimental data obtained from X-ray diffraction (for details see ESI). Despite the distortion of the backbone, π-dimers (d = 3.567 Å) are observed along the b axis in the packing. These dimers are also engaged in π-stacking interactions (d = 3.735 Å) to form infinite π-columns.

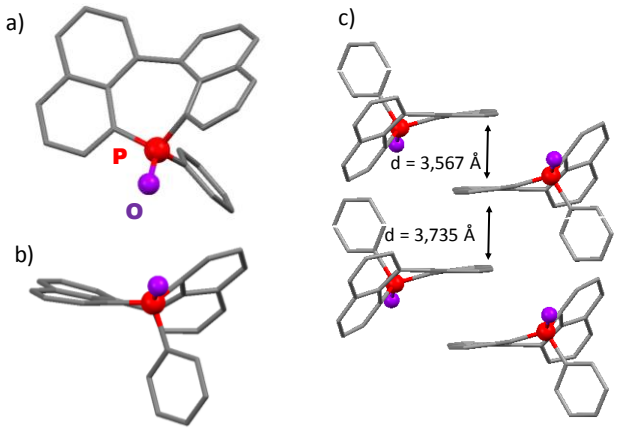
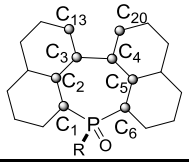


Figure 2: Top (a) and lateral (b) crystallographic views of **6**. Columns observed in the packing (c). Hydrogen atoms were omitted for clarity.

Table 1. Characteristic distances and angles taken from X-ray diffraction.



	6	8
P-C_1 (Å)	1.787	1.782
P-C_6 (Å)	1.801	1.777
C_1-C_2(Å)	1.442	1.426
C_2-C_3 (Å)	1.426	1.441
C_3-C_4 (Å)	1.513	1.514
C_4-C_5(Å)	1.422	1.445
C_5-C_6 (Å)	1.426	1.435
C_1-P-C_2(°)	110.98	107.54
C_{13}-C_3-C_4-C_{20}	38.88	30.40

Optical and redox properties

In order to further establish structure-property relationships in this novel family of π-conjugated P-heterocycles **6-8**, their UV-Vis absorption spectra were measured in CH_2Cl_2 (Fig. 3 and Fig. S17), as well as their fluorescence spectra were obtained both in solution and in solid-state and their cyclic voltammetry was measured in DMF with Bu_4NPF_6 as electrolyte (Table 1).

The UV-Vis absorption spectrum of the naphthyl-fused phosphepine **6** consists of a band with an absorption maximum centered at λ_{abs} = 346 nm (Fig. 3 and Table 1). This absorption is only weakly modified upon modification of the exocyclic P-R bond (for example, $\Delta\lambda$(**6**-**8**) = 5 nm, see Fig. S17 and Table 1). To get more insights into the optical properties of **6**-**9** TD-DFT calculations have been carried out at the B3LYP/6-31G*//B3LYP/6-31+G* level to obtain vertical excitation energies (see Table 2 for wavelengths and Table S9 for details).[8b] These calculations confirmed that the main transition observed in UV-vis absorption is between the HOMO and LUMO orbitals (Table S9). In compounds **6-8** the HOMO and LUMO orbitals are of π and π* type, respectively (Fig. 3 and Fig S22-23). In these orbitals the electron density is spread over the whole C-backbone, with no contribution of the P-atom in either the HOMO or the LUMO for all the computed structures (Fig. 3 and Fig. S22-23). Furthermore, the energy of these orbitals shows only a minor change upon substitution (Table 2), clearly explaining why the modification of the P-R bond only weakly affects the UV-vis absorption.

All phosphepines are good fluorophores with strong emission in the visible region in diluted solution. For example **6** displays a strong and unstructured emission in the visible region (λ_{em} (**6**) = 446 nm,ϕ = 46%, Fig 3). The remarkable Stoke shift of **6** is nicely reproduced by the TD-DFT calculations (6460 cm^{-1}) and the optimized geometry of the first excited state (S_1) indeed shows a significant distortion compared to that of that of the ground state (Fig. S24). In addition, naphthyl-fused phosphepines also display

luminescence in powder (Fig. 3 and Table 1) as illustrated for **6** that displays emission slightly blue-shifted compared to its emission in diluted solution (λ_{em} (**6**) = 424 nm with ϕ = 26% Fig. 4). This strong solid-state luminescence is a consequence of the distorted nature of the π-framework together with the presence of the tetrahedral P-atom which prevents efficient π-stacking and thus promote solid-state luminescence.[12]

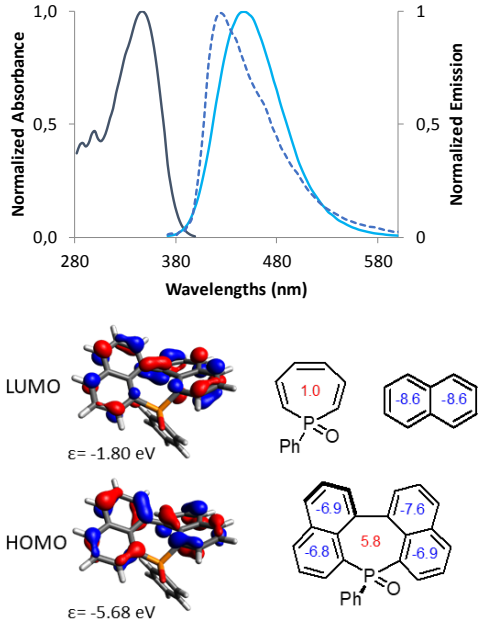


Figure 3: UV-vis absorption (dark blue) and emission (sky blue) in solution and powder (dotted line) of **6** in DCM (up); HOMO and LUMO of **6** calculated at the B3LYP/6-31G*//B3LYP/6-31+G* level (bottom, left); NICS(0) aromaticity patterns of oxa-phosphepine, naphthalene and **6** at the B3LYP/6-311+G**//B3LYP/6-31+G* level (bottom, right).

Regarding the redox properties, **6-8** displays no oxidation processes either in DCM or in DMF. However, a quasi-reversible reduction process is observed at -2.19 V vs Fc in DMF in the case of **6**. As expected, the reduction is not affected when the exocyclic P-R bond is modified (**7**-**8**, Table 1), in line with the similar LUMO energies of these compounds (see Table 2).

The aromatic character of the rings in the fused systems **6**-**8** has been investigated employing Nuclear Independent Chemical Shift (NICS) calculations at the B3LYP/6-311+G**//B3LYP6-31+G* level (Fig. 3). As an example, for **6** the seven-membered ring is anti-aromatic, while the naphthalene moieties of **6** globally retain their characteristic aromatic character.

OLEDs devices

Taking in account its thermal stability (td_{10} = 338°C) and its favorable electronic properties (*vide supra*), compound **6** was used as emitting material (EM) doped in 1,3-bis(N-carbazolyl)benzene (mCP) host in a multilayer OLED device (see exp. section). The performances of the OLED devices are reported in Table 3 and Fig. 4 for different concentrations of **6** in the mCP host. When the mCP matrix is doped with **6**, the emission spectra are changed from emission of mCP (main peak at 404 nm) to the emission of **6** (λ_{em} = 436 nm). From a doping rate of 1.5 %, we can note that the energy transfer from the host to the guest is complete. The devices emit a deep blue color with low CIE (Commission internationale de l'éclairage) color coordinates. Interestingly, the efficiency of the devices is almost independent of the doping rate in the range 1.5 to 3.7% with external quantum efficiency (EQE) of 1.6%. For doping rate as high as 70%, the EQE drops to 0.7% with no significant change of the emission spectrum. This can be explained by the low charge transport of **6** which is detrimental to the efficiency of the device.

Table 2. Photophysical and redox data.

	λ_{abs} [a] (λ_{abs} DFT) [b] [nm]	ε [a] [L.mol^{-1}.cm^{-1}]	λ_{em} [a] (λ_{em} DFT) [b] [nm]	Φ_F [c]	λ_{em} [c] [nm]	Φ_F [d]	E^{red} [e] [V]	ε^{HOMO} [b] [eV]	ε^{LUMO} [b1 [eV]
6	346 (357)	14000	446 (464)	0.46	424	0.26	-2.19 [f]	-5.68	-1.80
7	346 (361)	10500	442 (453)	0.46	432	0.27	-2.20 [f]	-5.64	-1.82
8	351 (370)	14000	442 (458)	0.46	513	0.09	-2.18 [f]	-5.65	-1.91

[a] In CH_2Cl_2 (10^{-5}M). [b] Calculated at the B3LYP/6-31G*//B3LYP/6-31+G* level [c] Measured relative to quinine sulfate (H_2SO_4, 1 N), ϕ_{ref}= 0.546. [d] Measured in calibrated integrated sphere. [e] In DMF with $Bu_4N^+PF_6^-$ (0.2 M) at a scan rate of 100 mV.s^{-1}. Potentials vs Fc^+/Fc. [f] quasi-reversible process.

Table 3. OLEDs devices performances

Doping ratio [%]	Von[a] [V]	EQE[b] [%]	cd/A[b]	Peak[c] [nm]	CIE (x; y)[b]
0	4.6	0.7	0.4	404	0.167; 0.110
1.5	4.1	1.6	0.9	436	0.151; 0.075
2.6	4.1	1.6	1.0	436	0.151; 0.077
3.1	4.3	1.5	0.9	436	0.150; 0.083
3.7	4.2	1.6	1.1	436	0.150; 0.086
70	3.7	0.7	0.5	436	0.161; 0.092

[a] recorded at luminance of 0.1 cd/m^2, [b] recorded at 30 mA/cm^2, [c] main peak.

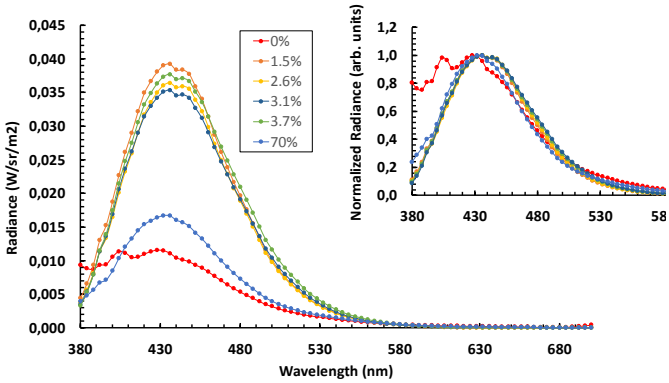


Figure 4: OLEDs spectra recorded at 30 mA/cm^2 for different doping rates. Insert shows the normalized spectra.

The performance of the best device (2.6% doping rate) is reported in Fig. S21 as a function of the current density. The maximum EQE is 1.65% and the maximum current efficiency is 1 cd/A at 2.5 mA/cm^2. The efficiencies drop at 20% from 0 to 50 mA/cm^2 in accordance with fluorescent OLEDs. The luminance is proportional to the current density with 400 cd/m^2 at current density of 50 mA/cm^2. Despite its modest device performances, these results are highly encouraging as this is, to our knowledge, the first insertion of a phosphepine-based emitter in an electroluminescent device. As 4, 5, and 6-membered P-rings have already been successfully inserted in OLEDs, these results confirm that π-conjugated P-heterocycles are highly appealing building blocks for lightning purpose.[1c,5,13]

Conclusions

In conclusion, the straightforward synthesis of a new family of naphthyl-fused phosphepines **6**-**8** has been described. This synthetic approach uses a chlorophosphine-oxide **3** that display strong resistance to hydrolysis due to a combination of steric shielding and pnictogenic interaction. The exocyclic P-R group can be easily tuned using the particular reactivity of **3**, opening the way toward functionalization of the compounds.[14] These derivatives display a highly distorted polycylic backbone. Photophysical studies revealed that these compounds are emissive in solution and in the solid-state. The successful incorporation of **6** into a blue emitting OLED confirmed that organosphorus derivatives in general, and π-extended phosphepines in particular, are appealing building blocks to design emitting materials for plastic electronics.

Experimental Section

General procedure. All experiments were performed under argon atmosphere using standard Schlenk techniques. Commercially available reagents were used as received without further purification. Solvents were freshly purified using MBRAUN SPS-800 drying columns. Separations were performed by gravity column chromatography on basic alumina (Aldrich, Type 5016A, 150 mesh, 58 Å) or silica gel (Merck Geduran 60, 0.063-0.200 mm). ^{1}H, ^{13} C, and ^{31}P NMR spectra were recorded on Bruker AV III 300 and 400 MHz NMR spectrometers equipped with BBO or BBFO probeheads. Assignment of proton and carbon atoms is based on COSY, NOESY, edited-HSQC and HMBC experiments. ^{1}H and ^{13}C NMR chemical shifts were reported in parts per million (ppm) using residual solvent signal as reference. In the NMR description. High-resolution mass spectra were obtained on a Varian MAT 311 or ZabSpec TOF Micromass instrument at CRMPO (Scanmat, UMS 2001). UV-Visible spectra were recorded rt on a VARIAN Cary 5000 spectrophotometer. The UV-Vis emission and excitation spectra measurements were recorded on a FL 920 Edimburgh Instrument equipped with a Hamamatsu R5509-73 photomultiplier for the NIR domain (300-1700 nm) and corrected for the response of the photomultiplier. Quantum yields in solution were calculated relative to quinine sulfate (H_2SO_4, 0.1 M), ϕ_{ref}= 0.55. The absolute quantum yields were measured with a C9920-03 Hamamatsu. The electrochemical studies were carried out under argon using an Eco ChemieAutolab PGSTAT 30 potentiostat for cyclic voltammetry with the three-electrode configuration: the working electrode was a platinum disk, the reference electrode was a saturated calomel electrode and the counter-electrode a platinum wire. All potential were internally referenced to the ferrocene/ ferrocenium couple. For the measurements, concentrations of 10^{-3} M of the electroactive species were used in freshly distilled and degassed DMF and 0.2 M tetrabutylammoniumhexafluorophosphate. Thermogravimetric Analysis were performed by using a Mettler-Toledo TGA-DSC-1 apparatus under dry nitrogen flow at a heating rate of 10 °C/min.

Experimental part. **2**. 1,8-Dibromonaphtalene (2 g, 7.1mmol, 3 eq) is dissolved in 80 mL of dry Et_2O. The solution is cooled down to -80°C then BuLi (2.8 mL, 7.1mmol, 3 eq) is added dropwise and the solution is stirred for 30 mn at -80°C then 30 mn at rt. The solution is again cooled down to -80°C and Ph_2PCl (0.423 mg, 2.37mmol, 1 eq) is added dropwise. The mixture is then stirred at RT overnight. Then the solution is quenched with 16 mL of water. 25 mL of DCM are then added then 4 mL of H_2O_2. After 2h of stirring, the solution is extracted with water and evaporated. The crude mixture was purified by silica gel chromatography using DCM/Et_2O (85/15) to afford **2** as a white powder (1.29 g, 99 %) ^{1}H NMR (400MHz, CD_2Cl_2, 243K): 8.11-8.02 (m, 4H), 7.99-7.94 (m, 3H), 7.84 (dd, *J* = 8 Hz, *J* = 2 Hz, 1H), 7.67-7.52 (m, 3H), 7.48-7.30 (m, 6H).^{13}C NMR (100 MHz, CD_2Cl_2, 273K): 138.0 (d, $J_{C\text{-}P}$ = 150 Hz, C_q),137.9 (d, J $_{C\text{-}P}$ = 14 Hz, CH), 137.4 (d, $J_{C\text{-}P}$ = 12 Hz, CH), 137.0 (d, $J_{C\text{-}P}$ = 7 Hz, C_q), 135.0 (d, $J_{C\text{-}P}$ = 60 Hz, CH), 133.9 (d, $J_{C\text{-}P}$ = 6 Hz, CH), 132.6 (d, J $_{C\text{-}P}$ = 260 Hz, C_q), 132.4 (d, J $_{C\text{-}P}$ = 2 Hz, C_q), 132.4 (s, CH), 131.3 (s, CH), 129.5 (d, J $_{C\text{-}P}$ = 53 Hz, CH), 126.8 (d, $J_{C\text{-}P}$= 17Hz, CH), 124.2 (d, $J_{C\text{-}P}$ = 15 Hz, CH), 120.2 (s, C_q).^{31}P NMR (162 MHz, CD_2Cl_2) δ +42.9. HRMS (ESI, CH_3OH / CH_2Cl_2: 9/1) : $[M+Na]^+$ ($C_{26}H_{17}ONaBr_2P$) m/z Calcd for : 556.9276. m/z Found : 556.9274. Anal. Calcd for $C_{26}H_{17}Br_2OP.2H_2O$: C, 54.57; H, 3.70. Found: C, 53.77; H, 3.07.

3. 1,8-Dibromonaphtalene (300 mg, 1.06 mmol, 4 eq) is dissolved in 20 mL of dry Et_2O. The solution is cooled down to -80°C then BuLi (0.42 mL, 1.06 mmol, 4 eq) is added dropwise and the solution is stirred for 30 mn at -80°C then 30 mn at rt. The solution is again cooled down to -80°C and PCl_3 (37 mg, 0.27 mmol, 1 eq) is added dropwise. The mixture is then stirred at RT overnight. Then the solution is quenched with 4 mL of water. 6 mL of DCM are then added then 1 mL of H_2O_2. After 2h of stirring, the

solution is extracted with water and evaporated. The crude mixture was purified by silica gel chromatography using DCM/Et_2O (85/15) to afford **3** as a white powder (134 mg, 99 %).^{1}H NMR (400 MHz, CD_2Cl_2, 223K): 8.90 (ddd, *J* = 20.1 Hz, *J* = 7.5 Hz, *J* = 2 Hz, 1H), 8.22-8.13 (m, 2H), 8.09-8.02 (m, 2H), 7.94 (t, *J* = 8.1 Hz, 2H), 7.76-7.69 (m, 2H), 7.47-7.43 (m, 1H), 7.36-7.27 (m, 2H). ^{13}C NMR (100 MHz, CD_2Cl_2, 223K) δ 137.7 (d, *J* = 8.8 Hz), 136.6 (d, *J* = 10.5 Hz), 136.1 (d, *J* = 10.4 Hz), 135.6 (d, *J* = 20.5 Hz), 135.3 (d, *J* = 3.5 Hz), 135.1 (d, *J* = 3.7 Hz), 131.9 (d, *J* = 5.6 Hz), 129.7 – 129.1 (m), 127.1 (d, *J* = 26.2 Hz), 124.6 (d, *J* = 15.8 Hz), 124.0 (d, *J* = 20.5 Hz), 119.0 (d, *J* = 6.0 Hz). ^{31}P NMR (162 MHz, CD_2Cl_2) δ +51.6. HRMS (ESI, CH_3OH / CH_2Cl_2 : 7/3) $[M+Na]^+$($C_{20}H_{12}OClBr_2PNa$) m/z calcd : 514.85732 m/z Found : 514.8572. Anal. Calcd for $C_{20}H_{12}Br_2ClOP$: found : C, 48.57; H, 2.45. Found: C, 48.04; H, 2.52.

4. (General method A). NaH (129 mg, 3.235 mmol, 4 eq) is dissolved in 40 mL of THF, then EtOH (149 mg, 3.235 mmol, 4 eq) is added at 0°C. After 1h30 stirring, **3** (400 mg, 0.809 mmol, 1 eq) is added at 0°C, and the reaction is stirred at RT 2 h. Then the solution is quenched with water, extracted with DCM and the solvents were evaporated. The crude mixture was purified by silica gel chromatography using DCM/Et_2O (9/1) to afford **4** as a white powder (320 mg, 78 %).^{1}H NMR (400 MHz, CD_2Cl_2, 293 K) δ 8,82-7.49 (m, 8H), 7.54-7.34 (m, 4H), 4.19-3.98 (m, 2H), 1.39-1.28 (m, 3H). ^{13}C NMR (101 MHz, CD_2Cl_2) δ 137.2 (s, C_q), 135.4 (s, CH), 134.5 (s, CH),133.6 (s, C_q), 129.8 (s CH*)*, 127.0 (s, C_q), 124.9 (d, J_{C-P} = 15.8 Hz, CH),120.4 (s, C_q), 62.1 (s, CH_2), 16.1 (d, J_{C-P} = 1.6 Hz, CH_3). 1C is not observable due to overlap. ^{31}P NMR (162 MHz, CD_2Cl_2) δ + 38.0. HRMS (ESI, CH_3OH / CH_2Cl_2 : 9/1) $[M+Na]^+$($C_{22}H_{17}OBr_2NaP$) m/z Calcd : 524.92251, m/z Found : 524.9224.

5. **5** was synthesized using General Method A with mesitol (396 mg, 2.91 mmol, 4 eq) and **3** (360 mg, 0.78 mmol, 1 eq) to afford **5** as white powder (320 mg, 78 %). ^{1}H NMR (400 MHz, CD_2Cl_2) δ 8.69-8.63 (m, 2H), 8.05 (d, 2H, J = 8.2 Hz), 7.9 (d, 2H, J = 8.2 Hz), 7.76 (d, 2H, J = 8.2 Hz), 7.50 (t, 2H, J = 7.5 Hz), 7.30 (t, 2H, J = 7.8 Hz), 6.81 (s, 2H) , 2.24 (s, 3H, Me) , 2.06 (s, 6H, Me).^{13}C NMR (101 MHz, CD_2Cl_2) δ 148.8 (s, C_q), 137.2 (d, J_{C-P} = 9.1 Hz, CH), 137.1 (d, J_{C-P} = 10.4 Hz, C_q), 134.9 (s, CH), 134.4 (d, J_{C-P} = 3.4 Hz, CH), 133.9 (d, J_{C-P} = 1.3 Hz, C_q), 133.6 (d, J_{C-P} = 8,1 Hz, C_q), 133.4 (d, J_{C-P} =142.6 Hz, C_q), 130.1 (d, J_{C-P} = 3.4 Hz, C_q), 130.0 (s, CH), 129.1 (d, J_{C-P} = 2.1 Hz, CH), 126.9 (s, CH), 125.0 (d, J_{C-P} = 15.4 Hz, CH), 120.1 (d, J_{C-P} = 5.1 Hz, C_q), 20.7 (s, Me) , 19.1 (s, Me).^{31}P NMR (162 MHz, CD_2Cl_2) δ +29.7.HRMS (ESI, CH_3OH) $[M+Na]^+$ ($C_{29}H_{23}Br_2NaO_2P$) (ESI, CH_3OH / CH_2Cl_2: 90/10) m/z Calcd : 614,96946 m/z Found : 614.9691.

6. (general method B) **2** (200 mg, 0.372 mmol, 1 eq) and 2,2 bipyridine (116 mg, 0.746 mmol, 2 eq) are dissolved in 400 mL of dry THF and degassed for 20 mn. COD (0.09, 0.746 mmol, 2 eq) and $Ni(COD)_2$ (206 mg, 0.746 mmol, 2 eq) are added and the solution is stirred overnight at 25°C then 20 mL of MeOH are added. The mixture is filtered on $MgSO_4$, washed with Et_2O and the THF is evaporated. The crude mixture was purified by silica gel chromatography using DCM/AcOEt (1/1) to afford **6** as a white powder (108 mg, 78 %). ^{1}H NMR (400 MHz, CD_2Cl_2) δ 8,77 (ddd, 2H, J = 14.4 Hz, J = 6.9 Hz, J = 1.4 Hz, H_8), 8.15 (d, 2H, J = 8.1 Hz, H_6), 7.95 (d, 2H, J = 7.7 Hz, $H_{2\ or\ 4}$), 7.75 (t, 2H, J = 7.4 Hz, H_7), 7.55-7.49 (m, 4H, H_3 and $H_{2or\ 4}$), 7.15-7.11 (m, 1H, H_{para}), 6.95-6.99 (m, 2H, H_{meta}), 6.82-6.77 (m, 2H, H_{ortho}). ^{13}C NMR (101 MHz, CD_2Cl_2) δ 140.1 (d, J_{C-P} = 2,0 Hz, C_1), 137.6 (d, J_{C-P} = 118 Hz, C_{ipso}), 136.1 (s, CH), 134.7 (d, J_{C-P} = 4,5 Hz, C_8), 133.9 (d, J_{C-P} = 2,9 Hz, C_6), 133.8 (d, J_{C-P} = 10,1 Hz, C_5), 132.1 (d, J_{C-P} = 11,4 Hz, C_{10}), 131.0 (d, J_{C-P} = 2,3 Hz, C_{para}), 130.1 (s, CH), 130.1 (d, J_{C-P} = 10,4 Hz, C_{ortho}), 128.5 (d, J_{C-P} = 12,1 Hz C_9), 128.1(d, J_{C-P} = 12,1 Hz, C_{meta}), 126.7 (s, CH),125.6 (d, J_{C-P} = 12.1 Hz, C_7). ^{31}P NMR (162 MHz, CD_2Cl_2) δ +22.7.HRMS (ESI, CH_3CN / CH_2Cl_2 : 80/20) $[M+H]^+$($C_{26}H_{18}OP$) m/z Calcd : 377.10898 m/z Found : 377.1088. Anal. Calcd for $C_{26}H_{17}OP$: C, 82.97 ; H, 4.55 . Found: C, 81.39; H, 4.62.

7. General method B was used using **4** (100 mg, 0.198 mmol, 1 eq) The crude mixture was purified by silica gel chromatography using DCM/AcOEt (1/1) to afford **7** as a white powder (36 mg, 53 %).^{1}H NMR (400 MHz, CD_2Cl_2) δ 8,58 (ddd, 2H, J = 14.9 Hz, J = 6.9 Hz, J = 1.5 Hz, H_8), 8.15 (d, 2H, J = 8.1 Hz, H_6), 7.97 (d, 2H, J = 7.7 Hz, $H_{2\ or\ 4}$), 7.69-7.61 (m, 6H, H_7, H_3 and $H_{2\ or\ 4}$), 3.03 (q, 2H, , J = 7.2 Hz, H_{11}), 0.55 (t, 3H, J = 7.5 Hz, H_{12}). ^{13}C NMR (101 MHz, CD_2Cl_2) δ140.5 (d, J_{C-P} = 1.9 Hz, C_q), 136.2 (s, C_7),134.3 (d, J_{C-P} = 3.0 Hz, C_6), 134.1 (d, J_{C-P} = 11.5 Hz, C_q), 134.1 (d, J_{C-P} = 5.8 Hz, C_8), 132.2 (d, J_{C-P} = 11.6 Hz, C_q), 130.0 (d, J_{C-P} = 1.8 Hz, $C_{2or\ 4}$), 127.6 (d, J_{C-P} = 129.5 Hz, C_9), 126.8 (s, $C_{3\ or\ 7}$),125.1 (d, J_{C-P} = 13.5 Hz, C_{3or7}), 60.2 (s, CH_2), 15.8 (d, J_{C-P} = 1.6 Hz, CH_3). ^{31}P NMR (162 MHz, CD_2Cl_2): δ +27.2.HRMS (ESI, CH_3OH / CH_2Cl_2: 9/1) $[M+Na]^+$($C_{22}H_{17}O_2NaP$) m/z Calcd : 367.0854, m/z Found : 367.0857.

8. General Method B was used with **5** (65 mg, 0.109 mmol, 1 eq) to afford **8** as white powder (38 mg, 47 %). ^{1}H NMR (400 MHz, CD_2Cl_2) δ 8,58 (ddd, 2H, J = 15.3 Hz, J = 6.9 Hz, J = 1.5 Hz, H_8), 8.19 (d, 2H, J = 8.2 Hz, H_6), 8.00 (d, 2H, J = 8.0 Hz, $H_{2\ or\ 4}$), 7.75 (d, 2H, J = 7.5 Hz $H_{2\ or\ 4}$), 7.69-7.64 (m, 4H, H_7 and H_3), 6.58 (s, 2H, H_{14}),2.10 (s, 3H, H_{16}), 1.33 (s, 6H, H_{13}).^{13}C NMR (101 MHz, CD_2Cl_2) δ 146.5 (s, J_{C-P} = 10.0 Hz, C_{11}), 140.4 (d, J_{C-P} = 1.9 Hz, C_q), 136.4 (s, $C_{2\ or\ 4}$), 134.5 (d, J_{C-P} = 3.0 Hz, C_6), 134.4 (d, J_{C-P} = 11.6 Hz, C_q), 134.2 (d, J_{C-P} = 2.1 Hz, C_q), 133.4 (d, J_{C-P} = 6.2 Hz, C_8), 132.3 (d, J_{C-P} =11.7 Hz, C_q), 130.6 (d, J_{C-P} = 3.0 Hz, C_q), 130.1(d, J_{C-P} = 1.9 Hz, $C_{2\ or\ 4}$), 129.4 (d, J_{C-P} = 2.0 Hz, C_{14}), 128.2 (s, C_q), 127.0 (s, $C_{3\ or\ 7}$), 125.2 (d, J_{C-P} = 3.7 Hz, $C_{3\ or\ 7}$), 20.6 (s, C_{16}) , 17.2 (s, C_{13}).^{31}P NMR (162 MHz, CD_2Cl_2) δ + 28.1. HRMS (ESI, CH_3OH / CH_2Cl_2: 9/1) $[M+Na]^+$($C_{29}H_{23}O_2NaP$) m/z Calcd : 457.13279, Found: 457.131.

X-ray crystallography

Single crystals suitable for X-Ray crystal analysis were obtained by slow diffusion of vapours of pentane into a dichloromethane solution of the derivatives at rt. Single crystal data collection were performed at 150 K with an D8 Venture Bruker-AXS diffractometer with Mo-*K*α radiation (λ = 0.71073 Å). The structure was solved by dual-space algorithm using the *SHELXT* program, and then refined with full-matrix least-squares methods based on F^2(*SHELXL*). All non-hydrogen atoms were refined with anisotropic atomic displacement parameters. H atoms were finally included in their calculated positions and treated as riding on their parent atom with constrained thermal parameters.

Computational details.

The computations were performed with the Gaussian 09 program package.[15] All structures were optimised using the B3LYP, B3LYPD3 and ωB97XD functionals combined with the 6-31+G* basis set. At each of the optimised structures vibrational analysis was carried out to check that the stationary point located is a minimum of the potential energy hypersurface (no imaginary frequencies were obtained) or a transition state (one imaginary frequency). The Wiberg Bond Indices were calculated with the NBO program version 3.1.[16] The AIM analysis was obtained with the Multiwfn code.[17] The molecular orbitals were plotted with Avogadro program.[18]

OLEDs fabrication and characterisation

The OLED devices were fabricated onto indium tin oxide (ITO) glass substrates purchased from Xin Yang Technology (90 nm thick, sheet resistance of 15 Ω/ϒ). Prior to organic layer deposition, the ITO substrates were cleaned by sonication in a detergent solution, rinsed twice in de-ionized water and then in isopropanol solution and finally treated with UV-ozone during 15 minutes. The OLEDs stack used is: Glass / ITO / CuPc (10 nm) / α-NPB (40 nm) / EML (20 nm) / TmPyPB (40 nm) / LiF (1.2 nm) / Al (100 nm). Copper II phthalocyanine (CuPc) is used as hole injection layer (HIL), N, N'-Bis-(1-naphthalenyl)- N,N'-bis-phenyl-(1,1′-biphenyl)-4,4′-diamine (αNPB) as hole transport layer (HTL), 1,3,5-Tri(m-pyridin-3-ylphenyl) benzene,1,3,5-Tris(3-pyridyl-3-phenyl) benzene (TmPyPB) as electron transport layer (ETL), lithium fluoride as electron injection layer (EIL) and 100 nm of aluminum as the cathode,respectively. The emitting layer (EML) is a host-guest system of 20 nm thick with 1,3-Bis(*N*-carbazolyl)benzene(mCP) as the host and molecule **6** as the guest (doping ratio 0-70% weight). Organic layers were sequentially deposited onto the ITO substrate at a rate of 0.2 nm/s under high vacuum (10^{-7} mbar). The doping rate was controlled by simultaneous co-evaporation of the host and the dopant. An in-situ quartz crystal was used to monitor the thickness of the layer depositions with an accuracy of 5%. The active area of the devices defined by the Al cathode was 0.3 cm^2. The organic layers and the LiF/Al cathode were deposited in a one-step process without breaking the vacuum.

After deposition, all the measurements were performed at rt and under ambient atmosphere with no further encapsulation of devices. The current–voltage–luminance (I–V–L) characteristics of the devices were

measured with a regulated power supply (ACT100 Fontaine) combined with a multimeter (Keithley) and a 1 cm^2 area silicon calibrated photodiode (Hamamatsu). Electroluminescence (EL) spectra and chromaticity coordinates of the devices were recorded with a PR650 SpectraScan spectrophotometer, with a spectral resolution of 4 nm.

Acknowledgements

This work is supported by the Ministère de la Recherche et de l'Enseignement Supérieur, the CNRS, the Région Bretagne, the French National Research Agency (ANR Heterographene ANR-16-CE05-0003-01, ANR Fluohyb ANR-17-CE09-0020), OTKA NN 113772 and BME-Nanonotechnology FIKP grant of EMMI (BME FIKP-NAT), PICS SmartPAH (08062). Y. Molard and G. Taupier (Scanmat-UMS 2001) are thanked for luminescence quantum yields measurements.

Keywords:π-conjugated systems • P-heterocycles • Optical properties • DFT calculations • OLED

[1] (a) T. Baumgartner, R. Réau, *Chem. Rev.* **2006**, *106*, 4681-4727. (b) M. Hissler, P. W. Dyer, R. Réau, *Coord. Chem. Rev.* **2003**, *244*, 1-44; (c) D. Joly, P. A. Bouit, M. Hissler, *J. Mater. Chem. C* **2016**, *4*, 3686-3698. (d) M. Stolar, T. Baumgartner, *Chem. As. J.l* **2014**, *9*, 1212-1225.

[2] J. I. Bates, J. Dugal-Tessier, D. P. Gates, *Dalton Trans.* **2010**, *39*, 3151-3159.

[3](a) P.-A. Bouit, A. Escande, R. Szűcs, D. Szieberth, C. Lescop, L. Nyulászi, M. Hissler, R. Réau, *J. Am. Chem. Soc.* **2012**, *134*, 6524-6527 ; (b) H. Omori, S. Hiroto, Y. Takeda, H. Fliegl, S. Minakata, H. Shinokubo, *J. Am. Chem. Soc.* **2019**, 141124800-4805.

[4] (a) F. Mathey, *Chem. Rev.* **1988**, *88*, 429-453; (b) M. P. Duffy, W. Delaunay, P. A. Bouit, M. Hissler, *Chem. Soc. Rev.* **2016**, *45*, 5296-5310 ; (c) Y. Ren, T. Baumgartner, *Dalton Trans.* **2012**, *41*, 7792-7800 ; (d) Y. Matano, H. Imahori, *Org. Biomol. Chem.* **2009**, *7*, 1258-1271.

[5] H. Chen, S. Pascal, Z. Wang, P.-A. Bouit, Z. Wang, Y. Zhang, D. Tondelier, B. Geffroy, R. Réau, F. Mathey, Z. Duan, M. Hissler, *Chem. Eur. J.* **2014**, *20*, 9784-9793.

[6] (a) C. Müller, L. E. E. Broeckx, I. de Krom, J. J. M. Weemers, *Eur. J. Inorg. Chem.* **2013**, *2013*, 187-202; (b) E. Regulska, C. Romero-Nieto, *Dalton Trans.* **2018**, *47*, 10344-10359.

[7] (a) X. He, J. Borau-Garcia, A. Y. Y. Woo, S. Trudel, T. Baumgartner, *J. Am. Chem. Soc.* **2013**, *135*, 1137-1147 ; (b) Y. Ren, M. Sezen, F. Guo, F. Jäkle, Y.-L. Loo, *Chem. Sci.* **2016**, *7*, 4211-4219; (c) W. Winter,*Chem. Ber.* **1976**, 109, 1405-2419; (d) D. Wu, C. Hu, L. Q, Z. Duan, F. Mathey *Eur. J. Org. Chem*. **2019**, 10.1002/ejoc.201901165.

[8] a) V. Lyaskovskyy, R. J. A. van Dijk-Moes, S. Burck, W. I. Dzik, M. Lutz, A. W. Ehlers, J. C. Slootweg, B. de Bruin, K. Lammertsma, *Organometallics* **2013**, *32*, 363-373; (b) T. Delouche, A. Mocanu, T. Roisnel, R. Szűcs, E. Jacques, Z. Benkő, L. Nyulászi, P.-A. Bouit, M. Hissler, *Org. Lett.* **2019**, *21*, 802-806.

[9] K. Schickedanz, J. Radtke, M. Bolte, H.-W. Lerner, M. Wagner, *J. Am. Chem. Soc.* **2017**, *139*, 2842-2851.

[10] Note that similar values have been reported for pnictogen interactions previously: S. Zahn, R. Frank, E. Hey-Hawkins and B. Kirchner, *Chem. Eur. J.* **2011**, 17, 6034-6038.

[11] Pnictogen bonding similarly to other so-called σ-hole interactions (hydrogen bond, halogen bond, etc.) is chiefly electrostatic interaction with minor covalent character (charge transfer) arising between a pnictogen center and a Lewis base: (a) S. Scheiner, *Acc. Chem. Res.* **2013**, *46*, 280– 288, (b) J. Moilanen, C. Ganesamoorthy, M. S. Balakrishna, H. M. Tuononen, *Inorg. Chem.* **2009**, *48*, 6740– 6747. (c) S. Scheiner, Noncovalent forces, Springer, Cham, 2015.

[12] (a) Y. Hong, J. W. Y. Lam, B. Z. Tang, *Chem. Soc. Rev.***2011**, *40*, 5361-5388; (b) F. Riobé, R. Szűcs, P.-A. Bouit, D. Tondelier, B. Geffroy, F. Aparicio, J. Buendía, L. Sánchez, R. Réau, L. Nyulászi, M. Hissler, *Chem. Eur. J.* **2015**, *21*, 6547-6556.

[13] (a) C. Fave, T. Y. Cho, M. Hissler, C. W. Chen, T. Y. Luh, C. C. Wu and R. Réau, *J. Am. Chem. Soc.*, **2003**, 125, 9254; (b) P. Hindenberg, J. Zimmermann, G. Hernandez-Sosa, C. Romero-Nieto, *Dalton Trans.***2019**, 8, 7503-7508.

[14] Z. Wang, B. S. Gelfand, T. Baumgartner, *Angew. Chem. Int. Ed.* **2016**, *55*, 3481-3485.

[15] Gaussian 09, Revision E.01, M. J. Frisch, G. W. Trucks, H. B. Schlegel, G. E. Scuseria, M. A. Robb, J. R. Cheeseman, G. Scalmani, V. Barone, B. Mennucci, G. A. Petersson, H. Nakatsuji, M. Caricato, X. Li, H. P. Hratchian, A. F. Izmaylov, J. Bloino, G. Zheng, J. L. Sonnenberg, M. Hada, M. Ehara, K. Toyota, R. Fukuda, J. Hasegawa, M. Ishida, T. Nakajima, Y. Honda, O. Kitao, H. Nakai, T. Vreven, J. A. Montgomery, Jr., J. E. Peralta, F. Ogliaro, M. Bearpark, J. J. Heyd, E. Brothers, K. N. Kudin, V. N. Staroverov, T. Keith, R. Kobayashi, J. Normand, K. Raghavachari, A. Rendell, J. C. Burant, S. S. Iyengar, J. Tomasi, M. Cossi, N. Rega, J. M. Millam, M. Klene, J. E. Knox, J. B. Cross, V. Bakken, C. Adamo, J. Jaramillo, R. Gomperts, R. E. Stratmann, O. Yazyev, A. J. Austin, R. Cammi, C. Pomelli, J. W. Ochterski, R. L. Martin, K. Morokuma, V. G. Zakrzewski, G. A. Voth, P. Salvador, J. J. Dannenberg, S. Dapprich, A. D. Daniels, O. Farkas, J. B. Foresman, J. V. Ortiz, J. Cioslowski, and D. J. Fox, Gaussian, Inc., Wallingford CT, 2013

[16] NBO Version 3.1 by E. D. Glendening, A. E. Reed, J. E. Carpenter, F. Weinhold

[17] Lu, T.; Chen, F. *J. Comput. Chem.* **2012**, 33, 580-592

[18] https://avogadro.cc/